

Application of a bubble formation model to decompression sickness in fingerling salmon

D. E. YOUNT

Department of Physics and Astronomy, University of Hawaii, Honolulu, HI 96822

Yount DE. Application of a bubble formation model to decompression sickness in fingerling salmon. *Undersea Biomed Res* 1981; 8(4):199–208.—Recently a new cavitation model has been proposed in which bubble formation in aqueous media is initiated by spherical gas nuclei stabilized by surface-active membranes of varying gas permeability. In previous applications of the varying-permeability model, good agreement has been obtained with experimental limits in pressure reduction for gelatin, rats, and humans following steady-state exposures. We now extend this investigation to fingerling salmon and demonstrate that a satisfactory description of the decompression data of D'Aoust et al. (*Undersea Biomed Res* 1980; 7:199–209) is provided by the model with parameter values that are similar to those found for other physical and biological systems. This adds further evidence for the generality of the model as well as for the importance of bubble nucleation as the primary and controlling event in decompression sickness.

cavitation theory
bubble formation
salmonid fingerlings

decompression theory
supersaturation
surface-active membranes

With the development of the varying-permeability model (1, 2) it is now possible to describe quantitatively a wide range of cavitation phenomena. The model was originally derived from studies of bubble formation in transparent gelatin (3–6). Next it was shown (7) that the model could be used to predict limits in pressure reduction both in rats (8) and in humans (9). The model has also been used in a critique of the U.S. Navy's traditional decompression theory (10), in a review of the theory of the countercurrent diffusion phenomenon (11), and in an analysis of the effects that oxygen breathed at elevated partial pressures has on decompression outcomes (12).

The experiment of D'Aoust et al. (13) on fingerling salmon presents both an opportunity and a challenge. The opportunity is to demonstrate what the varying-permeability model can do when confronted by another system (the physostomatous fishes), and by a variety of inert gases (helium, neon, nitrogen, and argon). The challenge is to the model itself: Does it survive, and can it continue to serve as the basis for a new theory of exogenous gas bubble disease?

Independently of the varying-permeability model, it is of interest to examine carefully any of the more traditional interpretations that may apply. For example, D'Aoust et al. (13) have

stated that when the effects of the external supersaturation of the surrounding water are minimized, their experiment "reveals the original supersaturation:volume ratio concept used by Haldane [(14)]." The argument in the DISCUSSION section is that this statement is unwarranted, if not excluded, by the salmon data.

METHODS

According to the varying-permeability model (1,2), bubble formation in aqueous media is initiated mainly by spherical gas nuclei that are stabilized by elastic skins or membranes composed of surface-active molecules. Essentially the model is a description of the way nuclear radii respond to changes in ambient pressure. For a given pressure schedule one can calculate an initial minimum radius R_0^{\min} above which all nuclei originally present in the sample will ultimately grow to form macroscopic bubbles. Nuclear skins are ordinarily gas permeable and become impermeable only when subjected to large compressions, well above the 6 atm maximum increment used by D'Aoust et al. (13). The mechanical strength of the surfactant membrane is represented by the crumbling compression γ_c , which must exceed the surface tension γ for a permeable nucleus to survive. It follows in the ever-permeable region of the model that the number of bubbles N is uniquely associated with a radius R_0^{\min} and crumbling compression γ_c . More specifically, the isopleths of constant N satisfy a set of equations of the form (see Refs. 1, 2)

$$P_{ss} = 2\gamma(\gamma_c - \gamma)/R_0^{\min} \gamma_c + (\gamma/\gamma_c)P_{crush} \quad (1a)$$

where P_{crush} is the maximum overpressure or crushing pressure during compression and P_{ss} is the maximum supersaturation during decompression. Because the surface tension γ is poorly known in salmon, it is convenient to rewrite Eq. 1a as

$$P_{ss} = [1 - (\gamma/\gamma_c)](2\gamma/R_0^{\min}) + (\gamma/\gamma_c)P_{crush} \quad (1b)$$

and treat the quantities γ/γ_c and $2\gamma/R_0^{\min}$ as the two free parameters, rather than γ_c and R_0^{\min} per se.

Following the steps in Ref. 7, Eqs. 1a and 1b are applied to decompression sickness by assuming that a given physiological result is associated with a definite number of bubbles. The data of D'Aoust et al. (13) are presented in terms of dive scores averaged over groups of five fish each, where 0 = no effect, 1 = decompression sickness, and 2 = death. Because of the averaging protocol, intermediate scores such as 0.5 and 1.5 are possible. According to the model and auxiliary assumptions, each isopleth of constant dive score will correspond to a line of constant (though unknown) bubble number per unit volume in salmon and of constant γ/γ_c and $2\gamma/R_0^{\min}$ in Eq. 1b.

The fingerling salmon were compressed from atmospheric pressure $P_0 = 1$ atm abs to a maximum pressure P_1 at a rate of 50 ft/min (15.3 m/min). Subjects remained at P_1 for 90 min of saturation time, which corresponded to the maximum decompression effect that could be demonstrated. Decompression from P_1 to P_f (final pressure) took place at a rate of 100 ft/min (31 m/min), and fish were observed individually for a period of 30 min after decompression. Under these conditions, the maximum overpressure and supersaturation in Eqs. 1a and 1b are given, respectively, by

$$P_{crush} = P_1 - P_0 \quad (2a)$$

and

$$P_{ss} = P_1 - P_f \quad (2b)$$

Eq. 1b can now be rewritten as

$$P_i - P_f = [1 - (\gamma/\gamma_c)](2\gamma/R_0^{\min}) + (\gamma/\gamma_c)(P_i - P_0) \quad (3)$$

For a given dive score and set of parameter values γ/γ_c and $2\gamma/R_0^{\min}$, Eq. 3 predicts that the allowed supersaturation or limit of pressure reduction $P_i - P_f$ will increase linearly with the exposure pressure P_i . The result is a family of straight lines. If each of these lines is analyzed separately, two parameter values per dive score will be required. According to the varying-permeability model, however, γ/γ_c and $2\gamma/R_0^{\min}$ are related by an equation of the form (see Ref. 2)

$$\gamma_c/\gamma = 1 + \beta_0(R_0^{\min}/2\gamma) \quad (4)$$

where β_0 (determined mainly by the difference in chemical potential for a surfactant molecule in the nuclear skin and in the surrounding reservoir) is independent of the dive score or bubble number. When Eq. 4 is used to calculate γ/γ_c for each value of $2\gamma/R_0^{\min}$, a comprehensive description of a whole family of dive score data can be obtained by specifying one "family" parameter β_0 and only one "individual" parameter $2\gamma/R_0^{\min}$ per dive score or line. This method of analysis is adopted here to minimize the number of free parameters and to insure the internal consistency of the model predictions.

RESULTS

The limits of pressure reduction $P_i - P_f$ from D'Aoust et al. (Fig. 2 of Ref. 13) are shown as a function of exposure pressure P_i in Fig. 1. These data, taken with a mixture of 80% nitrogen and 20% oxygen, demonstrate the linear dependence predicted for permeable nuclei by Eq. 3. A useful measure of the agreement between the model predictions and the experimental limits of pressure reduction is provided by the "sample standard deviation from regression," which is defined (15) as the square root of the mean-squared deviation per degree of freedom. Since five dive scores are involved in Fig. 1, six parameter values are required— β_0 and five values of $2\gamma/R_0^{\min}$. With 23 data points, this leaves $23 - 6$, or 17 degrees of freedom. The sample standard deviation (SD) from regression for the data points in Fig. 1 is then

$$\sigma_{17} = \left(\sum_{i=1}^{23} \Delta_i^2 / 17 \right)^{1/2} \quad (5a)$$

$$= \pm 0.16 \text{ atm} \quad (5b)$$

The value of the parameter β_0 for this family of straight lines and for all of the calculations that follow is

$$\beta_0 = 0.60 \text{ atm} \quad (6)$$

The values of the individual dive score parameters are, respectively,

$$\text{score, } 2\gamma/R_0^{\min}, \gamma/\gamma_c = 0.0, 0.48 \text{ atm}, 0.44 \quad (7a)$$

$$= 0.5, 0.90 \text{ atm}, 0.60 \quad (7b)$$

$$= 1.0, 1.50 \text{ atm}, 0.71 \quad (7c)$$

$$= 1.5, 4.00 \text{ atm}, 0.87 \quad (7d)$$

$$= 2.0, 20.0 \text{ atm}, 0.97 \quad (7e)$$

Although the format of Fig. 1 is ideally suited to these purposes, it is also of interest to compare the model predictions with the data points as they were originally taken—i.e., as

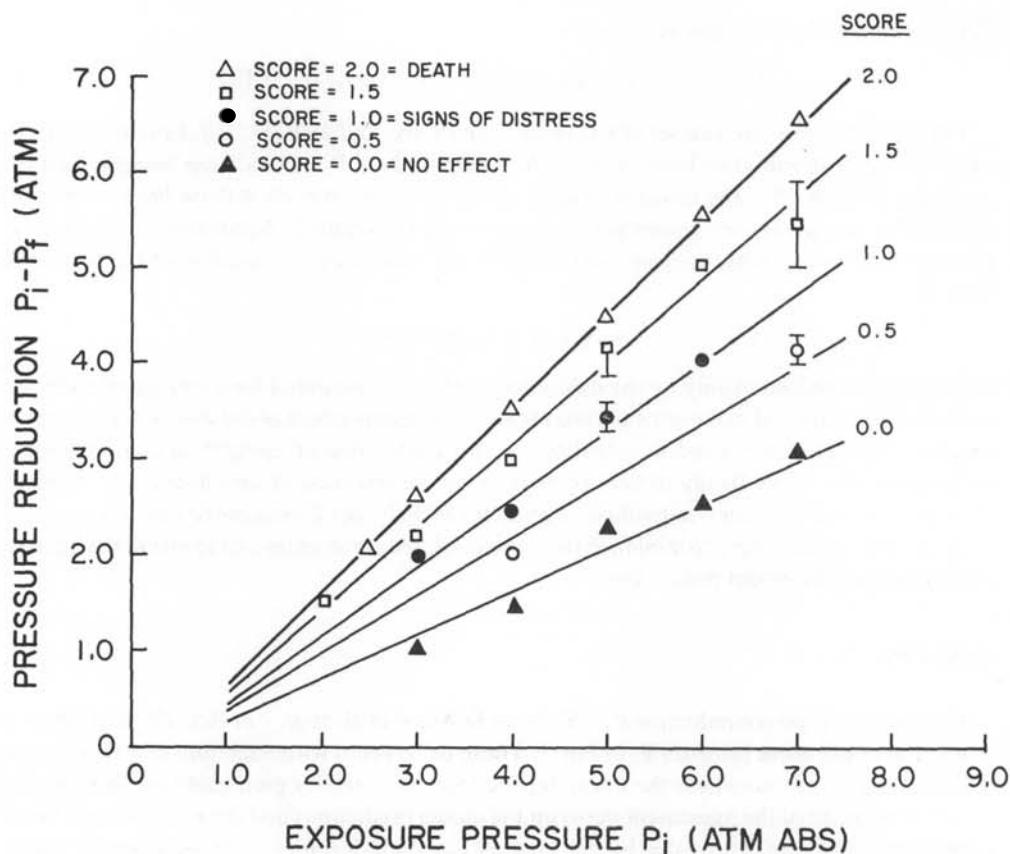


Fig. 1. Limits of pressure reduction $P_i - P_f$ vs. exposure pressure P_i for various dive scores in fingerling salmon. Data points obtained from D'Aoust et al. (Fig. 2 of Ref. 13); varying-permeability model predictions (solid lines) calculated from Eqs. 3 and 4, with $\beta_0 = 0.60$ atm.

dive scores for various combinations of P_i and $P_i - P_f$. This is done in Fig. 2. The data points and error bars were transcribed from D'Aoust et al. (Fig. 1 of Ref. 13), and the model predictions were read off from my Fig. 1. More specifically, for each dive score and exposure pressure P_i in Fig. 1, I merely read off the corresponding pressure reduction $P_i - P_f$. Since five scores were available, this gave five points for each exposure pressure plotted in Fig. 2. I then drew a smooth curve through each set of five points, noting that dive scores of 0.0 and 2.0 are limiting cases.

The fact that the "smooth" curves in Fig. 2 are wavy rather than straight is associated with the arbitrary trinomial scoring system (0 = no effect, 1 = decompression signs, and 2 = death) and has no special significance in the model. In particular, the number of bubbles corresponding to a given dive score is not determined by this analysis, and the primordial radial distribution $N(R_0^{\min})$ in fingerling salmon remains unknown. A related observation is that the assignment of error bars to dive scores by D'Aoust et al. (13) is rather imprecise, since the original measurements were restricted to a small number of discrete values 0, 1, and 2. This caveat does not apply to the analysis of the limits of pressure-reduction plotted in Fig. 1 because for a given dive score these limits vary continuously with exposure pressure (15).

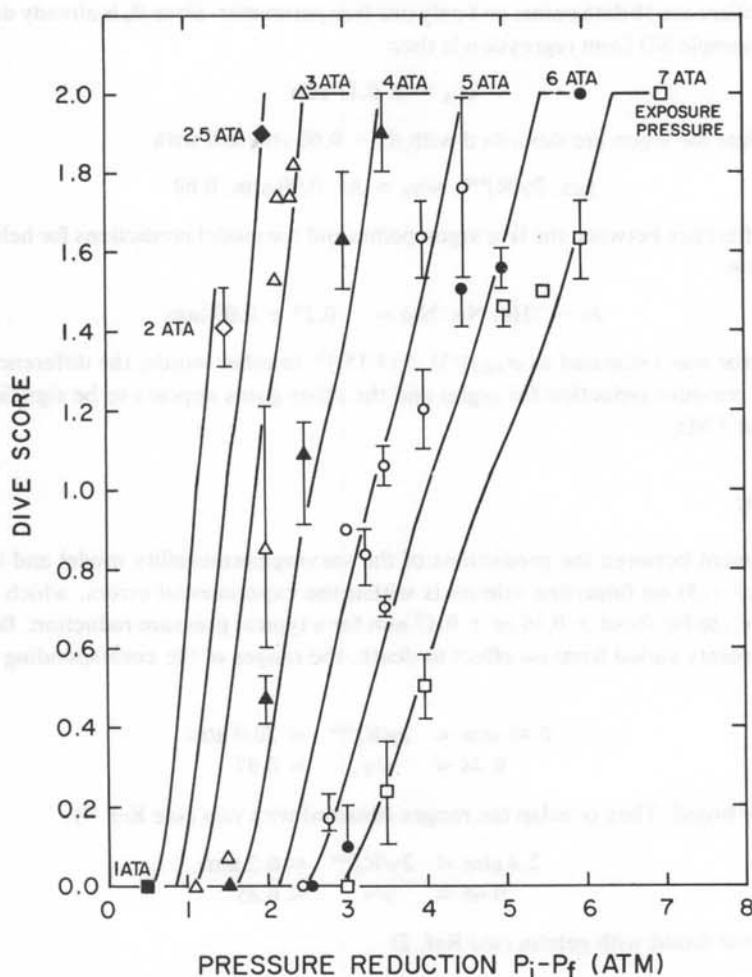


Fig. 2. Dive scores vs. pressure reduction $P_i - P_f$ for various exposure pressures P_i . These are original data points plotted by D'Aoust et al. (Fig. 1 of Ref. 13). The varying-permeability model predictions (solid lines) were read off from Fig. 1 of this paper. Within the experimental errors assigned by D'Aoust et al. (13), the agreement between the model and the data appears to be excellent.

D'Aoust et al. (13) obtained dive scores for four different inert gases—helium, neon, nitrogen, and argon—all mixed with 20% oxygen. In an effort to reduce the effects of a possible reverse transfer of gas from the surrounding supersaturated water to the supersaturated fish, some of these data were taken 15 min post-decompression, rather than the usual 30 min. The 40%–50% responses, compiled from D'Aoust et al. (Figs. 5a–d of Ref. 13) are plotted in Fig. 3.

There is no statistically significant difference in the limits of pressure reduction for helium, neon, and nitrogen in Fig. 3, and these points can be described by Eqs. 3 and 4 with β_0 again set equal to 0.60 atm and with individual parameter values, respectively, of

$$\text{gas, } 2\gamma/R_0^{\min}, \gamma/\gamma_c = \text{He, Ne, N}_2, 1.30 \text{ atm, } 0.68 \quad (8)$$

In this case, there are 16 data points and only one free parameter, since β_0 is already determined. The pooled sample SD from regression is then

$$\sigma_{15} = \pm 0.17 \text{ atm} \quad (9)$$

The data points for argon are described with $\beta_0 = 0.60 \text{ atm}$ and with

$$\text{gas}, 2\gamma/R_0^{\min}, \gamma/\gamma_c = \text{Ar}, 0.90 \text{ atm}, 0.60 \quad (10)$$

The mean difference between the five argon points and the model predictions for helium, neon, and nitrogen is

$$\text{Ar} - (\text{He}, \text{Ne}, \text{N}_2) = -0.27 \pm 0.09 \text{ atm} \quad (11)$$

where the error was estimated as $\sigma_{15}[(1/5) + (1/15)]^{1/2}$. In other words, the difference between the limits of pressure reduction for argon and the other gases appears to be significant at the level of about 3 SD.

DISCUSSION

The agreement between the predictions of the varying-permeability model and the data of D'Aoust et al. (13) on fingerling salmon is within the experimental errors, which I estimate from σ_{15} or σ_{17} to be about ± 0.16 or $\pm 0.17 \text{ atm}$ for a typical pressure reduction. Because the salmon end points varied from no effect to death, the ranges of the corresponding parameter values

$$0.48 \text{ atm} \leq 2\gamma/R_0^{\min} \leq 20.0 \text{ atm} \quad (12a)$$

$$0.44 \leq \gamma/\gamma_c \leq 0.97 \quad (12b)$$

are unusually broad. They overlap the ranges obtained with rats (see Ref. 7)

$$2.4 \text{ atm} \leq 2\gamma/R_0^{\min} \leq 6.2 \text{ atm} \quad (13a)$$

$$0.66 \leq \gamma/\gamma_c \leq 0.85 \quad (13b)$$

as well as those found with gelatin (see Ref. 2)

$$0.60 \text{ atm} \leq 2\gamma/R_0^{\min} \leq 4.4 \text{ atm} \quad (14a)$$

$$0.52 \leq \gamma/\gamma_c \leq 0.89 \quad (14b)$$

The parameter values for humans (see Ref. 7)

$$0.76 \text{ atm} \leq 2\gamma/R_0^{\min} \leq 0.90 \text{ atm} \quad (15a)$$

$$0.21 \leq \gamma/\gamma_c \leq 0.29 \quad (15b)$$

are compatible with the others but differ somewhat because the experimental end points covered a narrower range and were less severe. The conclusion from this comparison is that the varying-permeability model is readily applicable to the limited data available for physostomatous fishes and that such fishes are similar to mammals in their response to supersaturation stress.

The varying-permeability model is not, by itself, a theory of decompression sickness. At best, it correctly describes one step in the complex process that culminates in this disease syndrome. For example, there is nothing in the varying-permeability model per se that distinguishes between different gases at the same dissolved tension, even though it is well known that such differences can be of great importance in diving. This does not mean that the model is wrong or even that its application is limited to a few special cases. Rather, for each such application it is necessary to take into account any other steps or mechanisms that may be

involved. In this context, the data of D'Aoust et al. (13), like those of Berghage et al. (8) considered earlier (7), are of particular interest because they are dominated, though not entirely controlled, by the nucleation phenomenon.

This point is illustrated by the data in Fig. 3. Although the argon results lie only about 13% lower than those for helium, neon, and nitrogen, this difference appears to be both statistically and conceptually significant. In the context of the varying-permeability model, the lower limits for pressure reduction in argon imply *prima facie* that a smaller number of primary bubbles is required by argon to produce the given 40%–50% response in salmon 15 min post-decompression. Since argon is more than twice as soluble as any of the other three inert gases, the volume of argon that can be released from solution is potentially more than twice as large. This, in turn, could result in more extensive growth of primaries or, if bubble growth is limited (16), in more numerous secondaries (11, 17, 18), thereby amplifying the decompression stress. Since the outcome in either case would be closely correlated with the number of primaries, a good description of the argon data would still be provided by the varying-permeability model, albeit with a different primary bubble number N and hence with different values of the model parameters $2\gamma/R_0^{\min}$ and γ/γ_c . In gelatin (2) a 13% variation in the pressure reduction $P_i - P_f$ can easily change the bubble number N by more than a factor of 2. It is very plausible, therefore, that the total volume of released gas is the same for all of the gases in Fig. 3 and that the large differences in solubility are exactly balanced by compensating differences in N .

Whereas it has just been demonstrated that the critical-volume hypothesis *per se* is entirely consistent with the data of D'Aoust et al. (13) and with assumption of a critical bubble number,

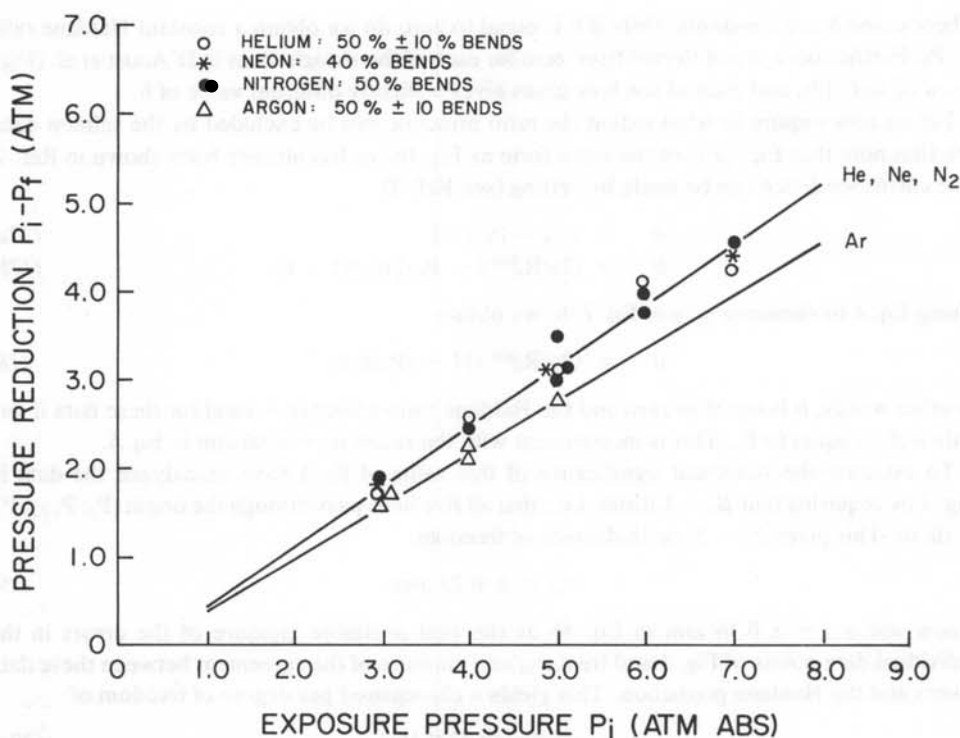


Fig. 3. Fifteen-minute post-decompression 40%–50% responses for helium, neon, nitrogen, and argon. Data points were compiled from D'Aoust et al. (Figs. 5a–d of Ref. 13), and the varying-permeability model predictions were obtained from Eqs. 3 and 4 with $\beta_0 = 0.60$ atm. The 13% difference between argon and the other three gases is statistically significant and may be associated with argon's greater solubility.

Hennessy and Hempleman (9) have shown that a family of straight lines similar to those in Figs. 1 and 3 can be derived from a critical-volume argument without taking nucleation into account. Instead, following Boycott et al. (14) and Hills (19), Hennessy and Hempleman (9) assume that "the whole excess of gas present in supersaturation were given off" (14). This implies an eventual "phase equilibration" between the dissolved gas and the released gas at the final pressure, and (unlike the application of the varying-permeability model) it leads to the prediction that both the slope and the intercept should depend strongly on the solubility. The absence of a strong dependence on inert gas in Fig. 3 is then evidence against equilibration and the formation of a large gas phase. Additional arguments opposing the derivation of Hennessy and Hempleman (9) are given in Ref. 7.

In their original Figs. 5a-d in Ref. 13, D'Aoust et al. plotted the 40%-50% responses for helium, neon, nitrogen, and argon separately, giving P_f as a function of P_i . Within the experimental errors this also yields a family of straight lines, motivating D'Aoust et al. (13) to assert that "examining the response at 15 min minimizes the effects of external supersaturation and reveals the original supersaturation:volume ratio concept used by Haldane [(14)], which can be clearly isolated with this animal model. Notice that each point on the line indicates a different ΔP !"

I believe that the foregoing statement of D'Aoust et al. (13) is unwarranted. The essential point is that a linear relationship between P_i and P_f does not necessarily imply a constant ratio P_i/P_f . Rather, it indicates that P_i and P_f are related by an equation of the form

$$P_i = a P_f + b \quad (16)$$

where a and b are constants. Only if b is equal to zero do we obtain a constant Haldane ratio P_i/P_f . Furthermore, b is different from zero for each of the straight lines in D'Aoust et al. (Figs. 5a-d of Ref. 13), and each of the four gases gives a slightly different value of b .

Let us now inquire to what extent the ratio principle can be excluded by the salmon data. We first note that Eq. 1a is of the same form as Eq. 16, as has already been shown in Ref. 7. The correspondence can be made by setting (see Ref. 7)

$$a = 1/[1 - (\gamma/\gamma_e)] \quad (17a)$$

$$b = (2\gamma/R_0^{\min}) - P_0/[(\gamma_e/\gamma) - 1] \quad (17b)$$

Using Eq. 4 to eliminate γ_e/γ in Eq. 17b, we obtain

$$b = (2\gamma/R_0^{\min}) [1 - (P_0/\beta_0)] \quad (18)$$

In other words, b is equal to zero and the Haldane ratio principle is valid for these data if and only if β_0 is equal to P_0 . This is inconsistent with the result $\beta_0 = 0.60$ atm in Eq. 6.

To estimate the statistical significance of this value of β_0 , I have reanalyzed the data in Fig. 1 by requiring that $\beta_0 = 1.0$ atm; i.e., that all five lines pass through the origin ($P_i, P_i - P_f$) = (0, 0). This gives 23 - 5, or 18 degrees of freedom.

$$\sigma_{18} = \pm 0.23 \text{ atm.} \quad (19)$$

I now use $\sigma_{17} = \pm 0.16$ atm in Eq. 5b as the best available measure of the errors in the individual data points of Fig. 1 and treat σ_{18} as a measure of the agreement between these data points and the Haldane prediction. This yields a chi-squared per degree of freedom of

$$\chi^2/\text{df} \sim (0.23/0.16)^2 \quad (20a)$$

$$\sim 2.2 \quad (20b)$$

The probability of obtaining a chi-squared per degree of freedom of 2.2 or larger with 18 degrees of freedom is less than 0.5%. Stating this result in another way, the salmon data favor the

varying-permeability model over the principle of the Haldane ratio by odds of greater than 200 to 1.

This discussion ends with a few remarks motivated by the last sentence in the above quotation by D'Aoust et al. (13). Whereas it is true in general that nucleation theory yields a pressure-difference (ΔP) principle (20) rather than a pressure-ratio (P_i/P_r) principle (14), this does not mean that the allowed pressure reductions ΔP will be independent of the earlier pressure history. On the contrary, Harvey (20) pointed out long ago that bubble formation could be strongly inhibited by a variety of methods, including the application of static pressure. This effect is quantified and made more explicit by the varying-permeability model, which correctly predicts the linear increase in allowed pressure reduction $P_i - P_r$ observed at modest exposure pressures P_i in a variety of physical and biological systems.

It is a pleasure to thank my colleagues Ed Beckman, Claude Harvey, Don Hoffman, Carl Honig, Fred Kavanaugh, and Jon Pegg for useful discussions and for constructive comments during the preparation of this manuscript. This work is a result of research sponsored in part by the University of Hawaii Sea Grant College Program under Institutional Grant Number NA79AA-D-00085 from NOAA Office of Sea Grant, U.S. Department of Commerce.—*Manuscript received for publication March 1981; revision received July 1981.*

Yount DE. Application d'un modèle de formation de bulles à l'étude de la maladie de décompression chez les jeunes saumons. *Undersea Biomed Res* 1981;8(4): 199–208. Récemment, il a été proposé un nouveau modèle de cavitation dans lequel la formation de bulles en milieux aqueux est amorcée par des noyaux gazeux sphériques, stabilisés par des membranes tensio-actives et de perméabilité aux gaz variable. Dans des études antérieures, en appliquant le modèle à perméabilité variable, on avait obtenu une bonne corrélation avec les limites de réduction de pression déterminées expérimentalement, après des expositions jusqu'à l'état d'équilibre, dans le cas de la gélatine, du rat, et de l'homme. Nous étendons maintenant cette étude au jeune saumon et démontrons que ce modèle fournit une description satisfaisante des données concernant la décompression, rapportées par D'Aoust et al. (*Undersea Biomed Res* 1980; 7:199–209) avec pour paramètres des valeurs similaires à celles trouvées avec d'autres systèmes physiques et biologiques. Ceci est une autre preuve du caractère général du modèle, comme de l'importance de la nucléation de bulles en tant que phénomène primaire et déterminant dans la maladie de décompression.

theorie de la cavitation
formation de bulles
jeunes salmonides

theorie de la décompression
sursaturation
membranes tensio-actives

REFERENCES

1. Yount DE, Kunkle TD, D'Arrigo JS, Ingle FW, Yeung CM, Beckman EL. Stabilization of gas cavitation nuclei by surface-active compounds. *Aviat Space Environ Med* 1977; 48:185–191.
2. Yount DE. Skins of varying permeability: a stabilization mechanism for gas cavitation nuclei. *J Acoust Soc Am* 1979; 65:1429–1439.
3. Strauss RH. Bubble formation in gelatin: implications for prevention of decompression sickness. *Undersea Biomed Res* 1974; 1:169–174.
4. Strauss RH, Kunkle TD. Isobaric bubble growth: a consequence of alternating atmospheric gas. *Science* 1974; 186:443–444.
5. Yount DE, Strauss RH. Bubble formation in gelatin: a model for decompression sickness. *J Appl Physiol* 1976; 47:5081–5089.
6. Yount DE, Yeung CM, Ingle FW. Determination of the radii of gas cavitation nuclei by filtering gelatin. *J Acoust Soc Am* 1979; 65:1440–1450.
7. Yount DE. Application of a bubble formation model to decompression sickness in rats and humans. *Aviat Space Environ Med* 1979; 50:44–50.
8. Berghage TE, Gomez JA, Roa CE, Everson TR. Pressure-reduction limits for rats following steady-state exposures between 6 and 60 ATA. *Undersea Biomed Res* 1976; 3:261–271.
9. Hennessy TR, Hempleman HV. An examination of the critical released gas volume concept of decompression sickness. *Proc R Soc Lond Biol* 1977; 197:299–313.

10. Yount DE. Responses to the twelve assumptions presently used for calculating decompression schedules. The Seventeenth Undersea Medical Society Workshop. Decompression theory. UMS Publ. No. 29WS (DT) 6-25-80. Bethesda: Undersea Medical Society, Inc., 1978:143-160.
11. Yount DE. Multiple inert-gas bubble disease: a review of the theory. ONR/UMS workshop on isobaric counterdiffusion. University of Pennsylvania (in press).
12. Yount DE, Lally DA. On the use of oxygen to facilitate decompression. *Aviat Space Environ Med* 1980; 51:544-550.
13. D'Aoust BG, Stayton L, Smith LS. Separation of basic parameters of decompression using fingerling salmon. *Undersea Biomed Res* 1980; 7:199-209.
14. Boycott AE, Damant GCC, Haldane JS. The prevention of compressed air illness. *J Hyg (Camb)* 1908; 8:342-443.
15. Snedecor GW, Cochran WG. Statistical methods. Ames: The Iowa State University Press, 1967:132-139.
16. Rubissow GJ, Mackay RS. Decompression study and control using ultrasonics. *Aerosp Med* 1974; 45:473-478.
17. Albano G. Principles and observations on the physiology of the scuba diver. English translation: ONR Report DR-150, Arlington, VA: Office of Naval Research, Department of the Navy, 1970:207-274.
18. Cowley JRM, Allegra C, Lambertsen CJ. Measurement of subcutaneous tissue pressure during superficial isobaric gas counterdiffusion. *J Appl Physiol: Respir Environ Exercise Physiol* 1979; 47:224-227.
19. Hills BA. A thermodynamic and kinetic approach to decompression sickness. Ph.D. Thesis. Adelaide: Library Board of South Australia, 1966.
20. Harvey EN. Physical factors in bubble formation. In: Fulton JS, ed. Decompression sickness. Philadelphia: W.B. Saunders & Co., 1951:90-114.